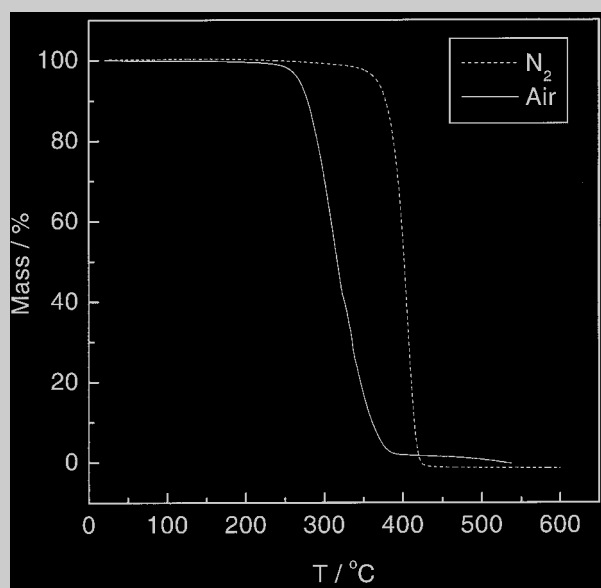


Full Paper: The thermal degradations of polystyrene (PS), polyethylene (PE), and poly(propylene) (PP) have been studied in both inert nitrogen and air atmospheres by using thermogravimetry and differential scanning calorimetry. The model-free isoconversional method has been employed to calculate activation energies as a function of the extent of degradation. The obtained dependencies are interpreted in terms of degradation mechanisms. Under nitrogen, the thermal degradation of polymers follows a random scission pathway that has an activation energy $\approx 200 \text{ kJ} \cdot \text{mol}^{-1}$ for PS and 240 and $250 \text{ kJ} \cdot \text{mol}^{-1}$ for PE and PP, respectively. Lower values ($\approx 150 \text{ kJ} \cdot \text{mol}^{-1}$) are observed for the initial stages of the thermal degradation of PE and PS; this suggests that degradation is initiated at weak links. In air, the thermoxidative degradation occurs via a pathway that involves decomposition of polymer peroxide and exhibits an activation energy of $125 \text{ kJ} \cdot \text{mol}^{-1}$ for PS and 80 and $90 \text{ kJ} \cdot \text{mol}^{-1}$, for PE and PP respectively.



TGA curves for the thermal decomposition of PS in nitrogen (dashed line) and air (solid line). Heating rates of 9.0 and $8.2 \text{ K} \cdot \text{min}^{-1}$ for nitrogen and air, respectively.

Kinetics of the Thermal and Thermo-Oxidative Degradation of Polystyrene, Polyethylene and Poly(propylene)

Jeffery D. Peterson, Sergey Vyazovkin,* Charles A. Wight*

Center for Thermal Analysis, Department of Chemistry, University of Utah, 315 S. 1400 E., Salt Lake City, UT 84112, USA

Introduction

The thermal degradation of polymers has been at the center of thermal analysis studies for many years.^[1–8] Of special interest are the degradation kinetics under inert and oxidative atmospheres. Thermogravimetric analysis (TGA) is a common method to study the kinetics of polymer degradations. Differential scanning calorimetry (DSC) is also employed to elucidate the decomposition steps observed in the TGA data. Kinetic analysis may effectively assist in probing degradation mechanisms as well as in predicting the thermal stability of polymers.^[6] These goals are accomplished only when using proper methods for kinetic evaluations. There have been a number of studies that report activation energies of the thermal degradation of PE,^[9–17] PP,^[10, 11, 18–25] and PS^[11, 17, 26–35] (cf. Table 1).

Unfortunately, the reported values are not always consistent. Although such inconsistencies are usually explained by differences in polymeric materials, one should not forget that they may also be attributed to computational artifacts.^[36]

Most evaluations are performed by fitting kinetic data to various reaction models, which provide Arrhenius parameters whose reliability is subject to the proper choice of the reaction model. The application of this model-fitting procedure to a single heating rate curve gives rise to activation energies that may differ by over an order of magnitude by simply choosing different reaction models.^[37] These discrepancies are not evident when comparing the correlation coefficients of the Arrhenius plots, in that they remain nearly identical for each chosen model.^[37] Additionally, an adequate description of poly-

Table 1. Literature values of the activation energy for degradation of PE, PP, and PS.

Poly-mer	Atmosphere	E kJ · mol ⁻¹	Experiment	Ref.
PE	N ₂	147	Nonisothermal TGA	[9]
PE	N ₂	241	Nonisothermal TGA	[10]
PE	N ₂	221	Isothermal TGA	[11]
PE	N ₂	272	Nonisothermal TGA	[12]
PE	N ₂	214, 239, 200 ^{a)}	Nonisothermal TGA	[13]
PE	N ₂	262	Factor-jump TGA	[16]
PE	Vacuum	273	Factor-jump TGA	[16]
PE	He	268	Isothermal TGA	[14]
PE	He	262	Nonisothermal TGA	[14]
PE	He	260	Nonisothermal Pyrolyzer	[17]
PE	Air	53	Nonisothermal TGA	[15]
PP	N ₂	244	Nonisothermal TGA	[10]
PP	N ₂	216	Isothermal TGA	[11]
PP	N ₂	214	Nonisothermal TGA	[18]
PP	N ₂	160	Nonisothermal TGA	[22]
PP	N ₂	115–200 ^{b)}	Nonisothermal TGA	[19]
PP	N ₂	130–200 ^{b)}	Nonisothermal TGA	[23]
PP	N ₂	230	Factor-jump TGA	[19]
PP	Vacuum	257	Factor-jump TGA	[19]
PP	Ar	98, 328 ^{c)}	Nonisothermal TGA	[25]
PP	Air	67	Nonisothermal TGA	[18, 21]
PP	Air	102	Nonisothermal TGA	[22]
PP	Air	72	Isothermal TGA	[24]
PP	Air	80–190 ^{b)}	Nonisothermal TGA	[19]
PS	N ₂	204	Isothermal TGA	[11]
PS	N ₂	250	Nonisothermal TGA	[33]
PS	N ₂	203–218 ^{d)}	Nonisothermal TGA	[34]
PS	N ₂	220, 277, 187 ^{a)}	Nonisothermal TGA	[34]
PS	N ₂	188	Factor-jump TGA	[28]
PS	and vacuum			
PS	Vacuum	187	Isothermal TGA	[26]
PS	Vacuum	205	Isothermal TGA	[27]
PS	Vacuum	198 ^{e)}	Nonisothermal TGA	[31]
PS	He	322	Nonisothermal TGA	[29]
PS	He	203	Nonisothermal TGA	[35]
PS	He	180	Isothermal TGA	[30]
PS	He	235	Nonisothermal Pyrolyzer	[17]
PS	Air	129	Nonisothermal TGA	[31]
PS	O ₂	90	Factor-jump TGA	[28]

a) Three-step mechanism is assumed.

b) Increases with extent of degradation.

c) Two-step mechanism is assumed.

d) Varies with assumed reaction order.

e) Independent of extent of degradation.

mer degradation kinetics may require developing significantly more complex models than the currently used models of reaction order and autocatalysis.^[38]

In order to circumvent the problems associated with model-fitting, one may use model-free isoconversional methods^[6] for calculating activation energies. The isoconversional methods require using multiple heating rate data. The use of multiple heating rate data appears to be

critical for obtaining reliable kinetic data. For instance, Burnham^[39] has shown that model-fitting to multiple heating rate data gives activation energies similar to the values estimated by the isoconversional methods.

The isoconversional methods permit the effective activation energy of a process to be unambiguously estimated as a function of the extent of conversion. The method can be effectively applied to the overall^[36] as well as species-specific^[40] rate data. Analysis of the resulting dependence provides important clues about changes in reaction mechanism.^[36] Note that there are some kinetic factors such as surface area of a reacting sample that do not directly affect the activation energy, but the effective value of the preexponential factor, estimating of which may in principle provide additional mechanistic clues. However, the estimates of the preexponential factor tend to be strongly correlated with the activation energy via compensation effect,^[41] which makes the preexponential factor a dependent and, therefore, inferior parameter. For this reason the discussion of the degradation kinetics is traditionally focused on the activation energy.^[1–5] Following this tradition we concentrate on the analysis of the activation energy and its variations with the extent of conversion.

Recently, we have successfully applied the isoconversional analysis to elucidate the kinetics and mechanism of poly(methyl methacrylate) degradation in nitrogen and various oxidative atmospheres.^[42] In this work we apply the isoconversional method to study thermal and thermoxidative degradation of three major polymers: that is PP, PE, and PS. The purpose of this study is to provide trustworthy kinetic data complemented by mechanistic interpretations.

Experimental Part

All of the polymer samples were obtained from Aldrich. The average molecular weights of PP and PS were 12000 and 280000, respectively. The average molecular weight of PE was not provided. Thermogravimetric analysis (TGA) experiments were performed by using a Rheometric Scientific TGA 1000M+ apparatus. As suggested by the manufacturer, a temperature calibration test was conducted by running the standard calcium oxalate monohydrate sample. The PE sample was in powder form and was used as received. Both the PP and PS were received as brittle beads. The PP beads were sliced with a razor blade into thin, oblong particles prior to TGA analysis. The PS samples were prepared by crushing the larger beads into small pieces of fairly uniform size. Polymer samples of 1–2 mg were placed in aluminum pans and heated at nominal heating rates of 0.5–20 K · min⁻¹ up to 600 °C. The actual heating rates were calculated from temperature measurements made during the period of polymer decomposition. The experiments were conducted in flowing atmospheres of nitrogen and air at flow rates 100 ml · min⁻¹.

A Mettler-Toledo DSC821^e was used to conduct the DSC tests. Polymer samples weighing 2–4 mg were placed in

open aluminum pans and heated at $20 \text{ K} \cdot \text{min}^{-1}$ up to 600°C in the atmospheres of flowing air and nitrogen at flow rates of $80 \text{ ml} \cdot \text{min}^{-1}$.

Kinetic Analysis of TGA Data

The kinetics of polymer degradations are usually described by the basic kinetic equation^[6]

$$\frac{da}{dt} = k(T)f(a) \quad (1)$$

where a represents the extent of reaction ($a = 0-1$), t is time, $k(T)$ is the rate constant, and $f(a)$ is the reaction model, which describes the dependence of the reaction rate on the extent of reaction. The value of a is experimentally determined from TGA as a relative mass loss. In most cases the temperature dependence of $k(T)$ can be satisfactorily described by the Arrhenius equation, whose substitution into Equation (1) yields

$$\frac{da}{dt} = A \exp\left(\frac{-E}{RT}\right)f(a) \quad (2)$$

where E is the activation energy and A is the preexponential factor.

To evaluate a dependence of the effective activation energy on the extent of conversion, we used an advanced isoconversional method,^[43] which is based on the assumption that the reaction model is independent of the heating program, $T(t)$. According to this method, for a set of n experiments carried out at different heating programs, the activation energy is determined at any particular value of a by finding E_a which minimizes the function

$$\Phi(E_a) = \sum_{i=1}^n \sum_{j \neq i}^n \left(\frac{J[E_a, T_i(t_a)]}{J[E_a, T_j(t_a)]} - 1 \right)^2 \quad (3)$$

where the subscripts i and j represent ordinal numbers of two experiments performed under different heating programs. Henceforth, the subscript a denotes the values related to a given extent of conversion. In the original method,^[43] the integral is evaluated by Equation (4)

$$J[E_a, T_i(t_a)] \equiv \int_0^{t_a} \exp\left[\frac{-E_a}{RT_i(t)}\right] dt \quad (4)$$

The method is easily modified to more adequately account for a variation of the activation energy with the extent of conversion.^[44] This is accomplished by breaking the kinetic curves up into segments. The activation energy for each segment is determined from numerical integration of the $T(t)$ data over the segment,

$$J[E_a, T_i(t_a)] \equiv \int_{t_{a-\Delta a}}^{t_a} \exp\left[\frac{-E_a}{RT_i(t)}\right] dt \quad (5)$$

In Equation (5), a varies from $2\Delta a$ to $1 - \Delta a$ with a step $\Delta a = (m + 1)^{-1}$, where m is the number of the equidistant values of a chosen for the analysis (usually 10–50). The minimization procedure is repeated for each value of a to find the dependence of the activation energy on the extent of conversion. An advantage of the advanced isoconversional method is that it can be applied to study the kinetics under arbitrary temperature programs (e.g., under a linear heating program distorted by self-heating).^[43] An earlier described statistical procedure^[45] has been employed to estimate confidence limits for E_a . The values of E_a have been estimated from 5–6 experiments carried out at different heating rates. The typical magnitudes of the confidence intervals for these values have been 10–20%.

Results

TGA Data

Figure 1 shows the TGA scans of PS degraded in nitrogen and air. In nitrogen, PS degrades in a single step beginning at 250°C and ending at 500°C . In the presence of air, PS degrades primarily in a single step from 200 to 450°C . There also appears to be an additional small step that occurs in the temperature region $450-575^\circ\text{C}$.

Figure 2 shows TGA data of PE degraded in nitrogen and air. Under a nitrogen atmosphere, PE degrades in a single, smooth step that begins at about 350°C and reaches zero mass at 490°C . In air, however, the degradation curve contains some irregularities. A derivative plot of mass loss versus time (shown on temperature scale for ease of comparison) for the TGA data in air indicates

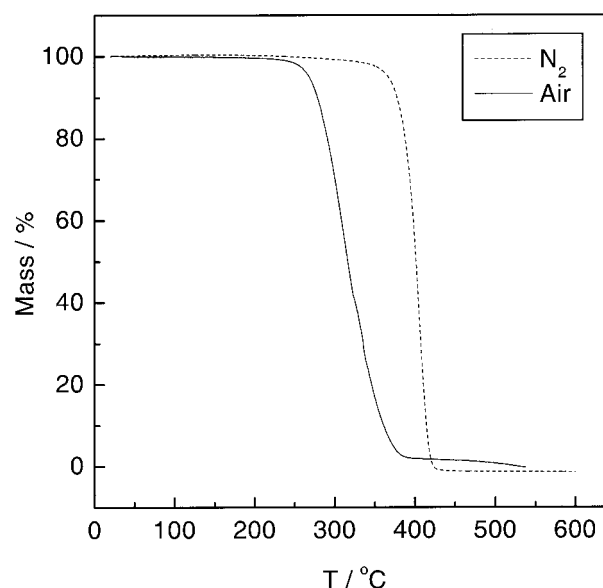


Figure 1. TGA curves for the thermal decomposition of PS in nitrogen (dashed line) and air (solid line). Heating rates of 9.0 and $8.2 \text{ K} \cdot \text{min}^{-1}$ for nitrogen and air, respectively.

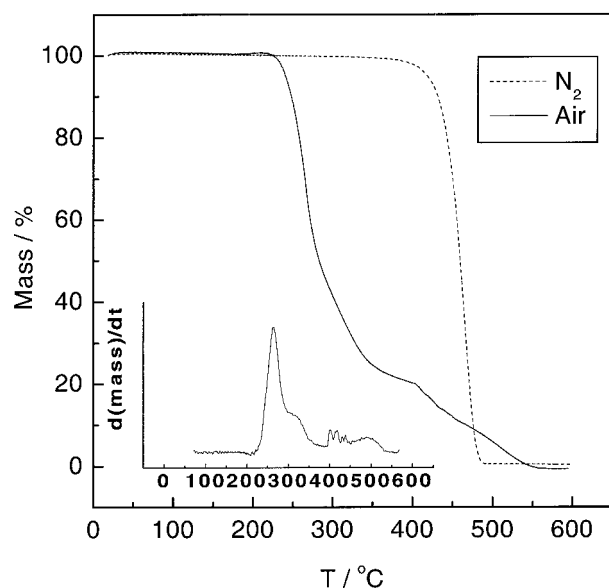


Figure 2. TGA curves for the thermal decomposition of PE in nitrogen (dashed line) and air (solid line). Inset plot is derivative graph of mass loss for degradation in air. Heating rates of 9.2 and 9.0 $\text{K} \cdot \text{min}^{-1}$ for nitrogen and air, respectively.

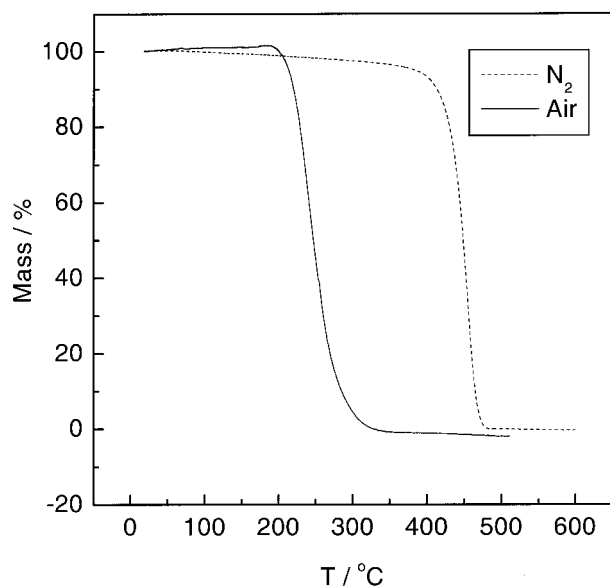


Figure 3. TGA curves for the thermal decomposition of PP in nitrogen (dashed line) and air (solid line). Heating rates of 9.1 and 8.2 $\text{K} \cdot \text{min}^{-1}$ for nitrogen and air, respectively.

numerous degradation steps (Figure 2 inset). The first is well defined and begins at $\approx 220^\circ\text{C}$. The second appears as a small shoulder at 320°C . A very irregular third peak arises from the sharp point in the TGA plot located at 400°C and continues smoothly above 475°C . Prior to any PE degradation, a slight increase in mass is detected under air at $\approx 200^\circ\text{C}$.

Figure 3 shows the TGA scans of PP degraded in nitrogen and air. Under nitrogen, the TGA curves indicate a

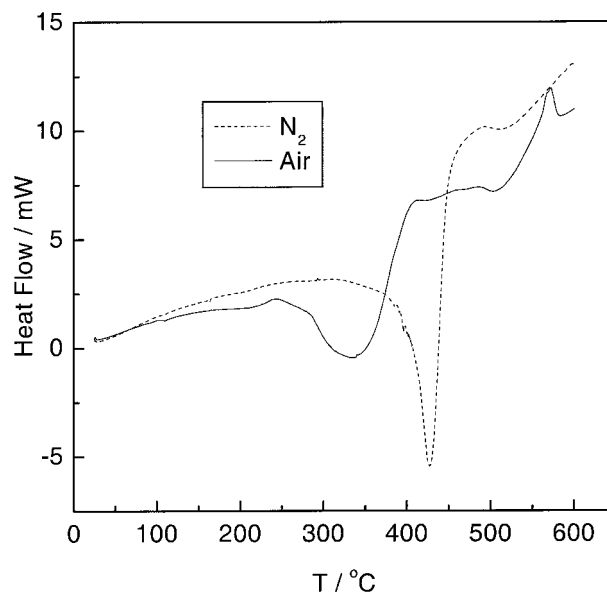


Figure 4. DSC scans of measured heat flow for degradation of PS in nitrogen (dashed line) and air (solid line). Heating rates of 20.0 $\text{K} \cdot \text{min}^{-1}$ for both nitrogen and air.

single degradation step that primarily occurs between 250 and 450°C . Like PE, PP also exhibits a similar mass increase ($\approx 180^\circ\text{C}$) prior to degradation under air. The oxidative degradation mostly occurs during the first step ($T = 200\text{--}450^\circ\text{C}$). This is followed by a minor mass loss step from 450 to 600°C .

Under both air and nitrogen, all polymer samples have degraded completely without leaving any noticeable residue.

DSC Data

The DSC traces for PS degradation are shown in Figure 4. The overall shape of the curves shows a slight increase in heat flow, followed by endotherms at 340°C and 430°C for degradations in air and nitrogen, respectively. The remaining curves then exhibit increases in heat flow until the degradation is complete at 600°C . There is also a small exothermic peak in the air trace located at 570°C .

The DSC traces of PE degraded in nitrogen and air are illustrated in Figure 5. Both curves show melting endotherms with a minimum at $\approx 110^\circ\text{C}$. After this point, however, the two scans differ significantly. In nitrogen, PE exhibits a broad endotherm that stretches up to $\approx 500^\circ\text{C}$. The minimum of the endotherm is found at 470°C . The DSC trace in air shows a large exothermic peak whose maximum is at 330°C . Immediately after this event, an extremely sharp exotherm is noticed at 410°C . The remaining signal is unstable, as evident by the numerous peaks and valleys.

The DSC traces for PP (Figure 6) is somewhat similar to those seen in PE. Melting endotherms are observed at

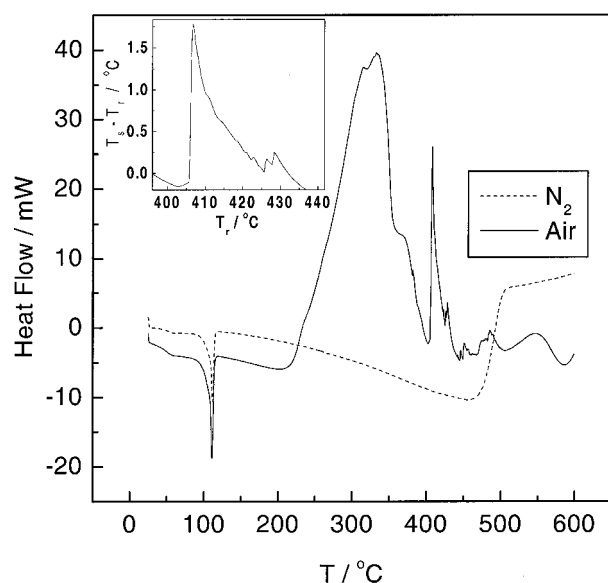


Figure 5. DSC scans of measured heat flow for degradation of PE in nitrogen (dashed line) and air (solid line). Heating rates of $20.0 \text{ K} \cdot \text{min}^{-1}$ for both nitrogen and air. Inset plot show the difference between sample temperature, T_s and reference temperature, T_r .

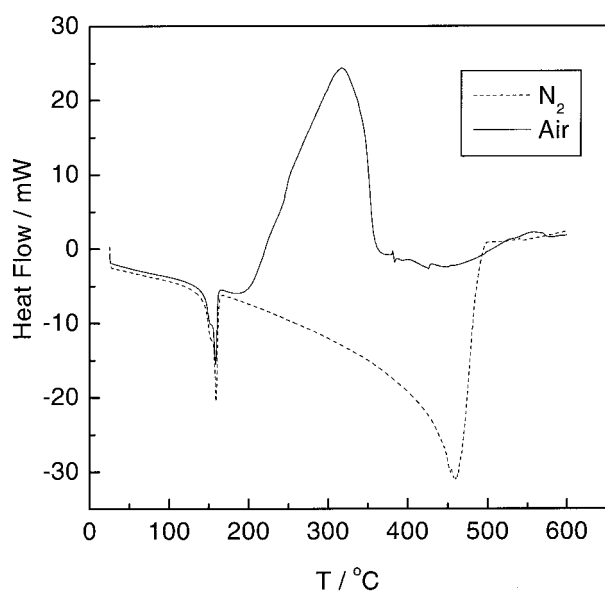


Figure 6. DSC scans of measured heat flow for degradation of PP in nitrogen (dashed line) and air (solid line). Heating rates of $20.0 \text{ K} \cdot \text{min}^{-1}$ for both nitrogen and air.

158°C . The remaining trace in nitrogen shows a broad endotherm with a minimum located at 460°C . In air, the DSC shows a large exothermic peak with a maximum at 316°C . However, unlike PE, the degradation of PP in air does not demonstrate the additional sharp exotherm.

Kinetic Data

The isoconversional activation energy plot for PS is shown in Figure 7. In a nitrogen environment, PS shows

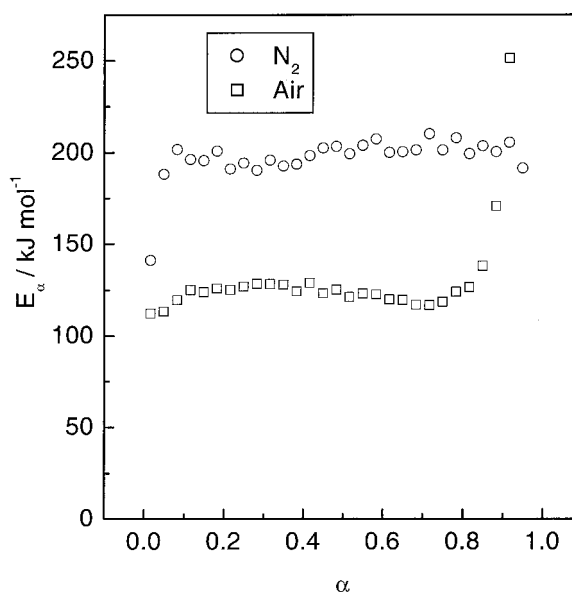


Figure 7. E_α -dependencies obtained by isoconversional analysis of TGA data for PS degradation in nitrogen (circles) and air (squares).

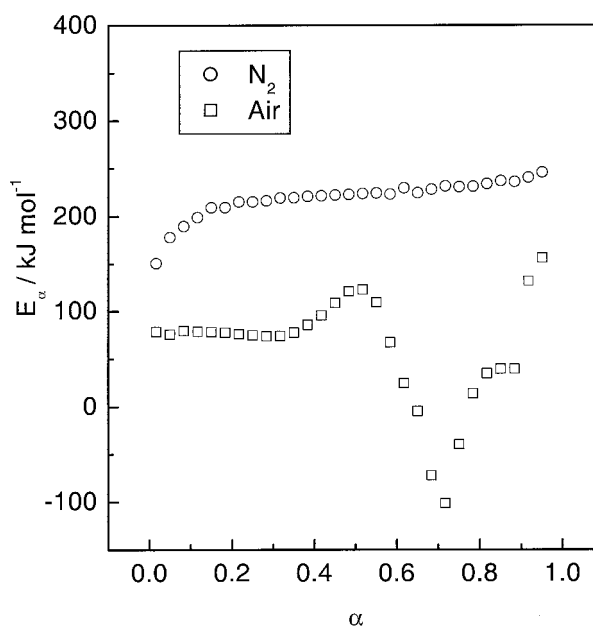


Figure 8. E_α -dependencies obtained by isoconversional analysis of TGA data for PE degradation in nitrogen (circles) and air (squares).

an activation energy of $\approx 200 \text{ kJ} \cdot \text{mol}^{-1}$, which is practically independent of the extent of degradation. When PS is degraded in air, the activation energy also remains fairly constant ($125 \text{ kJ} \cdot \text{mol}^{-1}$) throughout most of the degradation process ($\alpha < 0.85$).

An activation energy plot for PE is shown in Figure 8. In nitrogen, the activation energy moderately increases from 150 to $240 \text{ kJ} \cdot \text{mol}^{-1}$ throughout the degradation

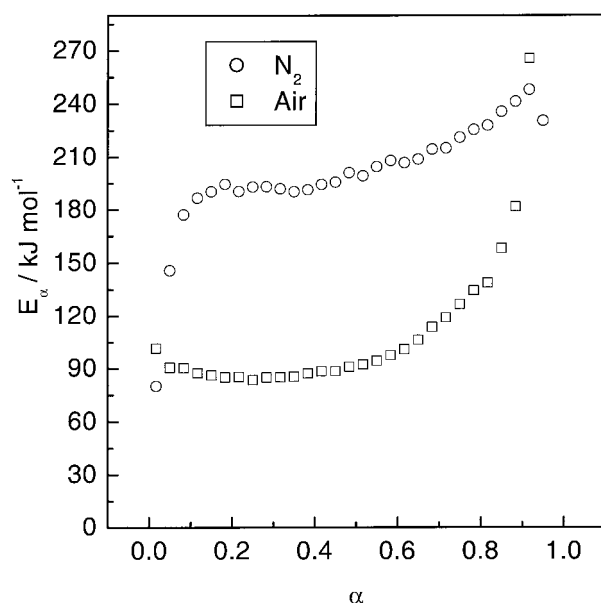


Figure 9. E_a -dependencies obtained by isoconversional analysis of TGA data for PP degradation in nitrogen (circles) and air (squares).

process. In air, the activation energy shows a slight increase from ≈ 80 to 125 during the initial degradation ($\alpha < 0.5$). The remaining reaction shows a highly unstable value of the activation energy.

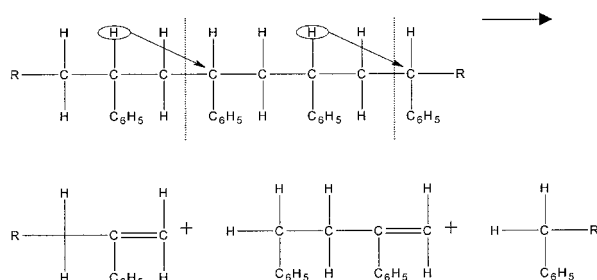
Figure 9 shows the activation energy dependence for degradation of PP in both nitrogen and air atmospheres. Under nitrogen, the degradation is characterized by a steadily increasing activation energy. Initial values of about $150 \text{ kJ} \cdot \text{mol}^{-1}$ occur at $\alpha = 0.05$ and increase to a maximum of $250 \text{ kJ} \cdot \text{mol}^{-1}$ at $\alpha = 0.9$. Under air, the degradation activation energy remains nearly constant at about $85 \text{ kJ} \cdot \text{mol}^{-1}$ during the first 40% of degradation, but steadily increases thereafter to a maximum of $270 \text{ kJ} \cdot \text{mol}^{-1}$ at $\alpha = 0.9$.

Discussion

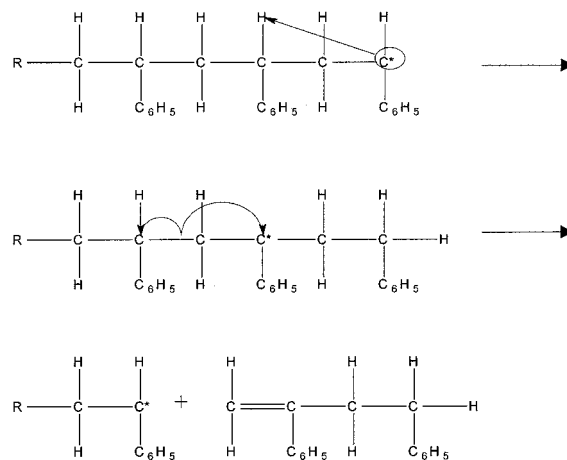
Thermal Degradation of Polystyrene

One of the earliest mechanisms of the thermal degradation of PS was proposed by Staudinger and Steinhöfer.^[46] In addition to monomer, the major degradation products consist of a mixture of saturated and unsaturated compounds, most of which were dimer and trimer. Staudinger and Steinhöfer proposed a chain scission mechanism to explain these products, as illustrated below for the PS dimer. Similar scission reactions would produce the monomer and trimer products as well.

Similarly, Grassie and Scott^[5] recognized the PS degradation products as being approximately 40% monomer, with decreasing amounts of dimer, trimer, tetramer, and pentamer. Their mechanism begins after thermal scission



produces two primary radical species. The reaction continues by producing a dimer via an intramolecular radical transfer reaction.



While typical depolymerization reactions are often described as unzipping, the above transfer reaction has been described as 'unbuttoning'.^[5]

It has been suggested by various authors that PS degradation is initiated at weak link sites inherent to the polymer itself.^[1,5] These sites arise during polymerization that is carried out in the presence of oxygen, which gives rise to peroxy^[5] and hydroperoxy^[1] structures. Once all of the weak-link sites have given way to initiation, the major mass loss of polymer occurs due to the random scission process described earlier.

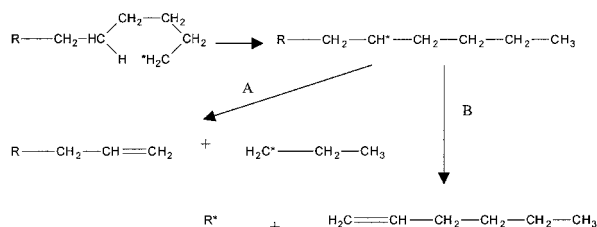
From the data in Figure 1, it is obvious that the PS sample degraded in a single step in nitrogen. The DSC data (Figure 4) show an endotherm, which is characteristic of typical depolymerization mechanisms. The DSC trace in nitrogen has a well-defined endothermic peak centered at 430°C , which is near the region of maximum mass loss in the TGA data.

The activation energy plot in Figure 7 gives an activation energy of $200 \text{ kJ} \cdot \text{mol}^{-1}$, which is nearly constant. The constancy of the value suggests that the degradation kinetics is essentially limited by a single reaction step, which appears to be unbuttoning initiated by random scission. The obtained result is in excellent agreement with data by Flynn,^[31] who also found the activation energy to be $\approx 200 \text{ kJ} \cdot \text{mol}^{-1}$ and independent of the extent of

degradation (Table 1). On the other hand, the majority of the values collected in Table 1 have been obtained by fitting data to single-step reaction models, which implicitly assumes the activation energy to be a constant value throughout the degradation. This type of analysis seems to be justified because the activation energy does not actually vary with the extent of reaction. For this reason most of the values reported in Table 1 appear to be reasonable and consistent.

Thermal Degradation of Polyethylene

The degradation mechanism of PE is much more complex than that of PS. First of all the unzipping process does not seem to be significant as very little monomer is produced (<1%). Instead, large amounts of hydrocarbons with anywhere from 1 to 70 carbon atoms are formed.^[5] Out of all these products, propene and 1-hexene appear to be the most abundant.^[5,47,48] This is due to the fact that a reaction of a radical with a hydrogen atom on the fifth carbon atom should be geometrically very favorable since the transition state is a six membered ring.^[5] The resulting radical species could then undergo chain scission producing two degradation pathways. As shown below, route A is responsible for the propene product, while B gives rise to 1-hexene.



The above mechanism begins at the weak link sites along the polymer chain once a thermally induced scission has occurred. There are four possible weak link structures within the PE chain, namely: peroxides, carbonyls, chain branches, and unsaturated structures. Grassie and Scott^[5] state that the true weak links in PE are probably peroxide groups formed during polymer preparation, storage and processing.

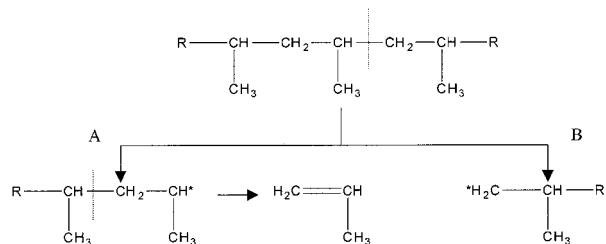
Although random scission is a primary degradation pathway in PE, it can also result in polymer chain branching.^[49] Both scission and branching occur simultaneously giving rise to a single mass loss step (Figure 2) and a single endotherm (Figure 5). The calculated activation energies for PE are shown in Figure 8. The observed variation in the activation energy suggests that the degradation kinetics is governed by different processes at the initial and final stages. The initial lower value of the activation energy is most likely associated with the initiation process that occurs at the weak links. As these weak links are consumed, the limiting step of degradation shifts

towards the degradation initiated by random scission, the mechanism of which has been described previously. This type of degradation typically has a greater activation energy. Therefore the maximum value of E_a ($\approx 240 \text{ kJ} \cdot \text{mol}^{-1}$, see Figure 8) gives us an estimate of the activation energy for the degradation initiated by random scission. This value is reasonably close to the value found for a similar process in PS.

Although we are not aware of other reports suggesting an increase in the activation energy with extent of degradation, Shlensky et al.^[50] observed the activation energy to significantly increase with temperature. Obviously this result also indicates a change in the limiting step of degradation. The change in the limiting step escapes kinetic analyses based on fitting experimental data to single-step reaction models, which force the activation energy to be constant. The resulting values can only be treated as the values averaged over the corresponding regions of temperature and extent of reaction. For this reason most of the reported values (Table 1) fit within the interval of variation in the activation energy found in the present work (Figure 8). Somewhat higher values may be caused by computational flaws of the method as well as by physical reasons. For instance, it is well known^[1] that the effective activation energy of PE degradation tends to increase with \bar{M}_w : $193 \text{ kJ} \cdot \text{mol}^{-1}$ (11000), $220 \text{ kJ} \cdot \text{mol}^{-1}$ (16000), and $277 \text{ kJ} \cdot \text{mol}^{-1}$ (23000). It is noteworthy that Conesa et al.^[13] assumed a three step degradation model that resulted in obtaining three different values of the activation energy all which also fit within the observed variation in E_a (Figure 8).

Thermal Degradation of Poly(propylene)

Like PE, the thermal degradation of PP occurs via random scission followed by radical transfer process. Unlike PE, however, PP degradation does not involve chain branching or crosslinking. The following scheme accounts for the formation of the most abundant degradation products.^[51–53] Pathway A proceeds via a secondary radical and produces the major products such as pentane (24.3%), 2-methyl-1-pentene (15.4%), and 2,4-dimethyl-1-heptene (18.9%). The primary radical of pathway B forms only minor products with 1.9% propane being the most abundant. All these processes occur simultaneously as evident by a single TGA mass loss step (Figure 3) and a single DSC endotherm (Figure 6).

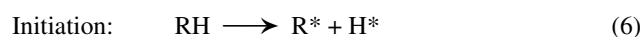


Although there is considerable agreement on the mechanism of PP degradation, there remains some inconsistencies in activation energies for this process. Table 1 gives values that range from 120 to 260 kJ · mol⁻¹. Since the structure and degradation mechanism is similar to that of PE one might expect to find a similar activation energy profile in PP. From Figure 9 we see that E_a increases with α from 150 to 250 kJ · mol⁻¹. The increase is obviously indicative of a change in the rate limiting step of the degradation kinetics. As in the case of PE, we assume the increase in the effective activation energy is caused by a shift of the rate limiting step from initiation to the degradation initiated by random scission, with respective estimates of the activation energy being 150 and 250 kJ · mol⁻¹. A similar increase has been reported by other workers.^[20, 23] By assuming a two-step degradation mechanism, Chan and Balke^[25] have obtained two significantly different values of the activation energy, which appear to lie outside the E_a variation found in the present study, as well as those reported by other workers.^[20, 23] Other values collected in Table 1 have been obtained by fitting data to single-step reaction models. This seems to be the reason why the change in the limiting step of the degradation was not detected. Again, these values of the activation energy should be treated as values averaged over the corresponding regions of temperature and extent of degradation.

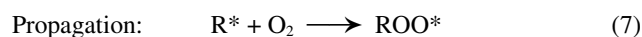
Thermo-Oxidative Degradation

While polymer degradations are more commonly studied in inert atmospheres, degradation in an oxygen environment is equally important. Thermo-oxidative degradation of polymers can provide practical, important information on how polymeric materials behave under more realistic atmospheric conditions. As noted by Flynn,^[54] thermal oxidation simplifies the kinetics because nearly all thermal oxidations of vinyl polymers at moderate temperatures are postulated to involve the hydroperoxide radical in the propagation step of the degradation. Because of this, most oxygen initiated depolymerizations have activation energies in the 80–110 kJ · mol⁻¹ range.

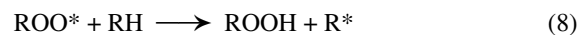
Degradation in oxygen begins via an initiation step which produces the radical precursors.



Initiation may be induced by physical (e.g., temperature, UV radiation, mechanical treatment) and/or chemical factors (e.g., traces of initiators such as peroxides and hydroperoxides used).^[55] When oxygen is allowed to react with the newly formed chain radical (R*), a peroxy radical intermediate is produced during the propagation step.

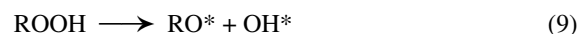


Highly reactive ROO* then abstracts a labile hydrogen from another polymer molecule giving rise to the hydroperoxide species, as well as another polymer radical, through which the process can continue.

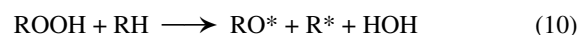


Grassie and Scott^[5] state that reaction (7) is a radical pairing process that has a low activation energy. Formation of the hydroperoxide in reaction (8) involves breaking a carbon-hydrogen bond and therefore, has a higher activation energy. In most polymers the rate of this step in the chain reaction determines the overall rate of oxidation. According to Reich and Stivala^[2] the activation energy of (8) is only about 30 kJ · mol⁻¹. They suggest that decomposition of the hydroperoxide plays a role of a limiting step in the overall kinetics of thermo-oxidative degradation of polymers.

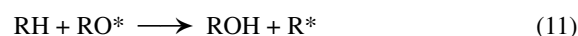
Monomolecular decomposition of hydroperoxides



should have a relatively high activation energy, which would be comparable to the energy of an O—O bond scission. For instance, the dissociation energy of hydrogen peroxide is ≈ 200 kJ · mol⁻¹.^[56] However, the relatively low activation energy experimentally obtained for decomposition of ROOH (105–125 kJ · mol⁻¹) suggests the following bimolecular decomposition mechanism



as a limiting step for thermoxidative degradation. The alkoxy radical, RO* can also effectively abstract hydrogen from the remaining polymer



Therefore, reaction (10) increases the concentration of the radical species involved in the propagation step (7), thereby accelerating oxidative degradation.

Polystyrene

The TGA data in Figure 1 of PS degradation indicates a single decomposition process that occurs between 250 and 400 °C. The fact that PS degrades at a lower temperature in air than it does in nitrogen is a property found in many polymers. This appears to occur as a result of switching the limiting step from random scission to decomposition of the hydroperoxide radical, which occurs with a lower activation energy.

According to the DSC data (Figure 4) the degradation under air is less endothermic. The decrease in the process endothermicity is apparently caused by the contribution from the exothermic reactions of the polymer oxidation. The integral thermal effect for the degradation in air is

$125.6 \text{ kJ} \cdot \text{mol}^{-1}$ ($T = 200\text{--}450$), as opposed to $241.5 \text{ kJ} \cdot \text{mol}^{-1}$ ($T = 250\text{--}500$) in nitrogen. The small exotherm at $\approx 575^\circ\text{C}$ is consistent with the small step of the mass loss (Figure 1) that occurs as a result of a complex process involving oxygen and PS degradation products as well as various carbon oxide species, which originate from thermo-oxidative degradation.^[57]

The activation energy remains fairly constant at about $120 \text{ kJ} \cdot \text{mol}^{-1}$ (Figure 7). The constancy of the value indicates that the whole degradation kinetics is essentially limited by a single reaction. The value of $120 \text{ kJ} \cdot \text{mol}^{-1}$ is consistent with values obtained^[56] for decomposition of peroxides (10) that suggest this reaction to be a limiting step of degradation. On the other hand, since the overall degradation remains endothermic under air, this suggests that the slow step of decomposition of the peroxoradical is followed by fast unzipping. This mechanism has been shown to occur using Fourier transform infrared spectroscopy.^[58]

Polyethylene

The TGA data shows (Figure 2) a small increase in the sample mass, which occurs prior to degradation. The increase is likely to be caused by the formation of a small amount of the polymer oxide. Because unzipping is insignificant in PE, the degradation process primarily occurs via reactions with oxygen. This results in the degradation becoming exothermic (Figure 5). The major degradation step ($T < 400^\circ\text{C}$) is followed by smaller mass loss step, which is observed as a change in the mass loss rate (Figure 2) and an exothermic spike in DSC (Figure 5). We assume that this exothermic event is caused by ignition of the sample. It is noteworthy that this event occurs at $\approx 400^\circ\text{C}$ independently of the heating rate. This temperature is quite consistent with the ignition temperatures of many carboxylic acids,^[59] which predominate at the later stages of degradation.^[5] The process is accompanied by a minor increase in the sample temperature (Figure 5) as measured by the DSC thermal sensor that touches the outside wall of the sample holder. Therefore, the sample surface temperature is likely to experience a larger increase in temperature that causes the mass loss rate to noticeably rise (Figure 2).

The occurrence of this exothermic event leads to unsteady degradation process, which is characterized by highly unstable values of the activation energy at $\alpha > 0.5$. The observed negative activation energies represent a computational artifact. The isoconversional method relies on data obtained at different heating rates. Normally, an increase in the heating rate causes a mass loss curve to shift to a higher temperature, which is consistent with a positive value of the activation energy. Conversely, the aforementioned thermal event does not show any systematic temperature shifts with the heating rate and

occurs rather randomly around 400°C . For this reason the activation energy also changes erratically around the extents of conversions related to this temperature region.

However, PE degradation demonstrates a practically constant value of $80 \text{ kJ} \cdot \text{mol}^{-1}$ during the first 40% of the reaction. The energy then increases slightly to about $125 \text{ kJ} \cdot \text{mol}^{-1}$. The obtained values agree well with the activation energies for the peroxide radical decomposition.^[56]

Poly(propylene)

Thermo-oxidative degradation of PP is quite similar to that of PE except that the exothermic reaction is steady. The degradation is preceded by a small increase in the sample mass (Figure 3). The overall process turns highly exothermic under air (Figure 6). The activation energy is fairly constant ($\approx 90 \text{ kJ} \cdot \text{mol}^{-1}$) during the first 40% of degradation (Figure 9), suggesting that the process kinetics is limited by a single reaction, which appears to be the peroxide radical decomposition. For the later degradation stages, the activation energy increases to values around $250 \text{ kJ} \cdot \text{mol}^{-1}$, which we also observed for the later stages of PP degradation under nitrogen (Figure 9). This suggests that the later stages of thermoxidative degradation are likely to occur via the same pathway that involves degradation initiated by random scission. Therefore, the thermoxidative degradation of PP appears to occur with a change in the limiting step from decomposition of peroxoradical to degradation initiated by random scission.

Conclusions

The isoconversional method has been applied to study the kinetics of the thermal and thermo-oxidative degradations of PS, PE, and PP. The method has yielded dependencies of the effective activation energy on the extent of polymer degradation. Under nitrogen, degradation of PS is characterized by a practically constant activation energy ($\approx 200 \text{ kJ} \cdot \text{mol}^{-1}$), whereas for degradation of PE and PP the activation energy increases with the extent of reaction ($150\text{--}240 \text{ kJ} \cdot \text{mol}^{-1}$ and $150\text{--}250 \text{ kJ} \cdot \text{mol}^{-1}$ for PE and PP, respectively). The initial lower values suggest the kinetics of the early degradation stages to be limited by initiation at the weak links. The higher values of the activation energy observed during the later stages indicate that decomposition of all three polymers becomes limited by degradation initiated by random scission.

Under air, the degradation of PS shows a practically constant activation energy $\approx 125 \text{ kJ} \cdot \text{mol}^{-1}$. The initial stages of thermo-oxidative degradation of PE and PP also show fairly constant activation energies of around $80\text{--}90 \text{ kJ} \cdot \text{mol}^{-1}$. These values agree well with the activation energies found for decomposition of peroxides, which suggests this process to be the rate limiting step of the

thermo-oxidative degradations. The later stages of PE degradation are obscured by a thermal event which appears to be polymer ignition. At the later stages of the thermo-oxidative degradation of PP, the activation energy significantly increases. This appears to be the result of a shift of the rate limiting step to degradation initiated by random scission.

Acknowledgement: The authors wish to thank the *Mettler-Toledo Company* for donating the DSC instrument that was used in this study. This research is supported by the *University of Utah Center for Simulations of Accidental Fires and Explosions (C-SAFE)*, funded by the *Department of Energy, Lawrence Livermore Laboratory*, under subcontract B341493.

Received: July 10, 2000
Revised: October 24, 2000

- [1] S. L. Madorsky, "Thermal Degradation of Organic Polymers", Interscience Publishers, New York 1964.
- [2] L. Reich, S. S. Stivala, "Elements of Polymer Degradation", McGraw-Hill, New York 1971.
- [3] W. Schnabel, "Polymer Degradation: Principles and Practical Applications", Macmillan, New York 1981.
- [4] T. Kelen, "Polymer Degradation", Van Nostrand, New York 1983.
- [5] N. Grassie, G. Scott, "Polymer Degradation and Stabilisation", Cambridge University Press, Cambridge 1985.
- [6] J. H. Flynn, "Thermal Analysis", in: *Encyclopedia of Polymer Science and Engineering*, Suppl. Vol., H. F. Mark, N. M. Bikales, C. V. Overberger, J. I. Kroschwitz, Eds., Wiley, New York 1989, p. 690.
- [7] "Handbook of Polymer Degradation", S. H. Hamid, M. B. Amin, A. G. Maadhah, Eds., M. Dekker, New York 1992.
- [8] "Degradation and Stabilization of Polymers: Theory and Practice", G. E. Zaikov, Ed., Nova Science Publishers, Commack, New York 1995.
- [9] Y. Cho, M. Shim, S. Kim, *Mater. Chem. Phys.* **1998**, 52, 94.
- [10] R. W. J. Westerhout, R. H. P. Balk, R. Meijer, J. A. M. Kuipers, W. P. M. van Swaaij, *Ind. Eng. Chem. Res.* **1997**, 36, 3360.
- [11] R. W. J. Westerhout, J. Waanders, J. A. M. Kuipers, W. P. M. van Swaaij, *Ind. Eng. Chem. Res.* **1997**, 36, 1955.
- [12] P. L. Beltrame, P. Carniti, G. Audisio, F. Bertini, *Polym. Degrad. Stabil.* **1989**, 26, 209.
- [13] J. A. Conesa, A. Marcilla, R. Font, J. A. Caballero, *J. Anal. Appl. Pyrolysis* **1996**, 36, 1.
- [14] H. Bockhorn, A. Hornung, U. Hornung, *J. Anal. Appl. Pyrol.* **1999**, 50, 77.
- [15] C. Vasile, E. Costea, L. Odochian, *Thermochim. Acta*, **1991**, 184, 305.
- [16] B. Dickens, *J. Polym. Sci., Polym. Chem. Ed.* **1982**, 20, 1065.
- [17] A. K. Burnham, R. L. Braun, *Energy Fuels* **1999**, 13, 1.
- [18] J. C. W. Chien, J. K. Y. Kiang, *Macromolecules* **1980**, 13, 280.
- [19] B. Dickens, *J. Polym. Sci., Polym. Chem. Ed.* **1982**, 20, 1169.
- [20] S. V. Vyazovkin, V. V. Bogdanova, I. A. Klimovtsova, A. I. Lesnikovich, *J. Appl. Polym. Sci.* **1991**, 42, 2095.
- [21] J. C. W. Chien, J. K. Y. Kiang, *Makromol. Chem.* **1980**, 181, 47.
- [22] J. Rychlý, L. Matisová-Rychlá, M. Vavreková, *J. Therm. Anal.* **1982**, 25, 423.
- [23] M. Day, J. D. Cooney, M. MacKinnon, *Polym. Degrad. Stab.* **1995**, 48, 341.
- [24] J. Rychlý, L. Matisová-Rychlá, K. Csmorova, L. Achimsky, L. Audouin, A. Tcharkhtchi, J. Verdu, *Polym. Degrad. Stabil.* **1997**, 58, 269.
- [25] J. H. Chan, S. T. Balke, *Polym. Degrad. Stabil.* **1997**, 57, 135.
- [26] H. H. G. Jellinek, *J. Polym. Sci.* **1949**, 4, 13.
- [27] L. A. Wall, S. Strauss, J. H. Flynn, D. McIntyre, *J. Phys. Chem.* **1966**, 70, 53.
- [28] B. Dickens, *Polym. Degrad. Stabil.* **1980**, 2, 249.
- [29] A. Tripathi, C. L. Vaughn, W. Maswadeh, H. L. Meuzelaar, *Energy Fuels* **1999**, 13, 984.
- [30] C. Bouster, P. Vermande, J. Veron, *J. Anal. Appl. Pyrol.* **1980**, 1, 297.
- [31] J. H. Flynn, *J. Therm. Anal.* **1988**, 34, 367.
- [32] F. Carrasco, P. Pages, *J. Appl. Polym. Sci.* **1996**, 61, 187.
- [33] X. Guoxi, L. Rui, T. Qinhua, L. Jinghua, *J. Appl. Polym. Sci.* **73**, 1139 (1999)
- [34] A. Marcilla, M. Beltrán, *Polym. Degrad. Stabil.* **1995**, 50, 117.
- [35] R. Lin, R. L. White, *J. Appl. Polym. Sci.* **1997**, 63, 1287.
- [36] S. Vyazovkin, C. A. Wight, *Int. Rev. Phys. Chem.* **1998**, 17, 407.
- [37] S. Vyazovkin, C. A. Wight, *Thermochim. Acta* **1999**, 340/341, 53.
- [38] B. J. McCoy, *Ind. Eng. Chem. Res.* **1999**, 38, 4531.
- [39] A. K. Burnham, *Thermochim. Acta* **2000**, 355, 165.
- [40] E. Bonnet, R. L. White, *Thermochim. Acta* **1998**, 311, 81.
- [41] S. Vyazovkin, W. Linert, *Int. Rev. Phys. Chem.* **1995**, 14, 355.
- [42] J. D. Peterson, S. Vyazovkin, C. A. Wight, *J. Phys. Chem. B* **1999**, 103, 8087.
- [43] S. Vyazovkin, *J. Comput. Chem.* **1997**, 18, 393.
- [44] S. Vyazovkin, *J. Comput. Chem.* **2001**, 22, 178.
- [45] S. Vyazovkin, C. A. Wight, *Anal. Chem.* **2000**, 72, 3171.
- [46] H. Staudinger, A. Steinhof, *Ann. Chem.* **1935**, 517, 35.
- [47] B. J. McGrattan, in: "Hyphenated Techniques in Polymer Characterization", T. Provder, M. W. Urban, H. G. Barth, Eds., American Chemical Society, Washington D.C. 1994.
- [48] D. E. Smith, *Thermochim. Acta* **1976**, 14, 370.
- [49] H. Hinsken, S. Moss, J. R. Pauquet, H. Zweifel, *Polym. Degrad. Stabil.* **1991**, 34, 279.
- [50] O. F. Shlensky, L. N. Aksenov, A. G. Shashkov, "Thermal decomposition of materials: effect of highly intensive heating", Elsevier, Amsterdam 1991.
- [51] Y. Tsuchiya, K. Sumi, *J. Polym. Sci. A*, **1969**, 7, 1599.
- [52] C. David, "Thermal Degradation of Polymers", in: *Comprehensive Chemical Kinetics*, vol. 14, C. H. Bamford, C. F. H. Tipper, Eds., Elsevier, Amsterdam 1975, p. 1.
- [53] Y. Tsuchiya, K. Sumi, *J. Polym. Sci. A* **1968**, 6, 415.
- [54] J. H. Flynn, "Polymer Degradation", in: *Handbook of Thermal Analysis and Calorimetry*, vol. 3, S. Z. D. Cheng, Ed., Elsevier, Amsterdam, in press.
- [55] J. F. Rabek, "Oxidative Degradation of Polymers", in: *Comprehensive Chemical Kinetics*, vol. 14, C. H. Bamford, C. F. H. Tipper, Eds., Elsevier, Amsterdam 1975, p. 425.
- [56] L. Reich, S. S. Stivala, "Autoxidation of hydrocarbons and polyolefins", M. Dekker, New York 1969, p. 50.
- [57] J. A. J. Jansen, J. H. Van der Maas, A. P. De Boer, *Appl. Spectrosc.* **1992**, 46, 88.
- [58] M. Celina, D. K. Ottesen, K. T. Gillen, R. L. Clough, *Polym. Degrad. Stabil.* **1997**, 58, 15.
- [59] "CRC Handbook of Chemistry and Physics", 78th edition, D. R. Laide, H. P. R. Frederikse, Eds., CRC Press, Cleveland, Ohio 1997.